

# Formation of Thioformic Acid (HCOSH)—The Simplest Thioacid—in Interstellar Ice Analogues

Jia Wang,<sup>#</sup> Joshua H. Marks,<sup>#</sup> Lotefa B. Tuli,<sup>#</sup> Alexander M. Mebel, Valeriy N. Azyazov, and Ralf I. Kaiser\*



Cite This: *J. Phys. Chem. A* 2022, 126, 9699–9708



Read Online

ACCESS |



Metrics & More

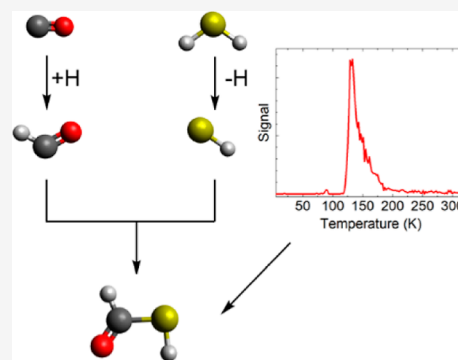


Article Recommendations



Supporting Information

**ABSTRACT:** Since the observation of the first sulfur-containing molecule, carbon monosulfide (CS), in the interstellar medium (ISM) half a century ago, sulfur-bearing species have attracted great attention from the astrochemistry, astrobiology, and planetary geology communities. Nevertheless, it is still not clear in which forms most of the sulfur resides in molecular clouds, an unsolved problem referred to as “sulfur depletion”. Reported herein is the formation of thioformic acid (HCOSH)—the simplest thioacid—in interstellar ice analogues containing carbon monoxide (CO) and hydrogen sulfide (H<sub>2</sub>S) at 5 K. Utilizing single photoionization reflectron time-of-flight mass spectrometry and isotopically labeled molecules, thioformic acid molecules were selectively photoionized in the temperature-programmed desorption phase. These studies unravel a key reaction pathway to thioformic acid, an organic molecule recently detected toward the giant molecular cloud G+0.693–0.027 and the hot core G31.41+0.31, thus shedding light on interstellar sulfur chemistry.



## 1. INTRODUCTION

Since the discovery of the first sulfur-containing molecule—carbon monosulfide (CS)—in the interstellar medium (ISM) half a century ago,<sup>1</sup> sulfur chemistry has attracted particular interest of the astrochemistry, astrobiology, and planetary geology communities.<sup>2</sup> To date, more than 270 molecules in interstellar and circumstellar regions have been reported,<sup>3</sup> 33 of which contain sulfur (Figure 1). These sulfur-bearing molecules include thiols, thioaldehydes, acids, and thioketenes/thiocumulenes. Interestingly, 13 new sulfur-bearing species have been identified within the last 5 years, accounting for about 40% of all known sulfur-bearing species. Sulfur-bearing compounds are detected in distinct astrophysical environments such as in the interstellar and intergalactic media, planetary surfaces, and icy moons.<sup>2</sup> These representative molecules are frequently used as tracers for the kinematics and chemical evolution of star- and planet-forming regions.<sup>4</sup> The detections of sulfur-bearing molecules motivate laboratory experiments on sulfur-containing interstellar ice analogues under simulated astrophysical conditions, which commonly involve reactions with atomic hydrogen,<sup>5,6</sup> thermal processing,<sup>7,8</sup> radiolysis with energetic electrons, protons, and helium ions,<sup>9</sup> photolysis exploiting photons ranging from visible light to X-rays,<sup>7,10</sup> and neutral–neutral gas-phase reactions.<sup>7,11,12</sup> However, it is not yet clear in which forms most of the sulfur resides in molecular clouds.<sup>13</sup> To solve this “missing sulfur” problem, systematic experimental studies under controlled chemical and physical conditions such as temperature, ice

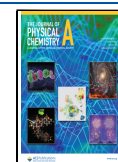
morphology, projectile ion-charge state, and energy are much needed.<sup>2</sup>

Very recently, thioformic acid (1, HCOSH) was detected toward the giant molecular cloud G+0.693–0.027, using both the IRAM 30 m telescope and the Yebes 40 m telescope,<sup>14</sup> as well as toward the hot core G31.41+0.31 in the GUAPOS spectral survey conducted with the ALMA interferometer.<sup>15</sup> Thioformic acid (1) exists in two stable planar conformations, *cis* and *trans* with respect to two hydrogen atoms. Rodríguez-Almeida et al. detected only the *trans* conformer in G+0.693–0.027 with a fractional abundance of  $(1.2 \pm 0.2) \times 10^{-10}$ , while the derived upper limit abundance of the *cis*-HCOSH conformer was less than  $0.2 \times 10^{-10}$ .<sup>14</sup> The column density and excitation temperature were  $(1.6 \pm 0.1) \times 10^{13}$  cm<sup>-2</sup> and  $10 \pm 1$  K, respectively.<sup>14</sup> Compared with its *cis* conformer, the *trans* conformer is 2.8 kJ mol<sup>-1</sup> more stable,<sup>15</sup> resulting in the equilibrium *trans/cis* ratio of 3:1 in the vapor phase at room temperature.<sup>16</sup> However, the pure excess of the detected *trans* conformer in this giant molecular cloud is particularly puzzling.<sup>17</sup> Following this question, García de la Concepción et al. searched for thioformic acid (1) conformers toward the hot core G31.41+0.31 to compare their abundances with the

**Received:** September 27, 2022

**Revised:** November 16, 2022

**Published:** December 19, 2022



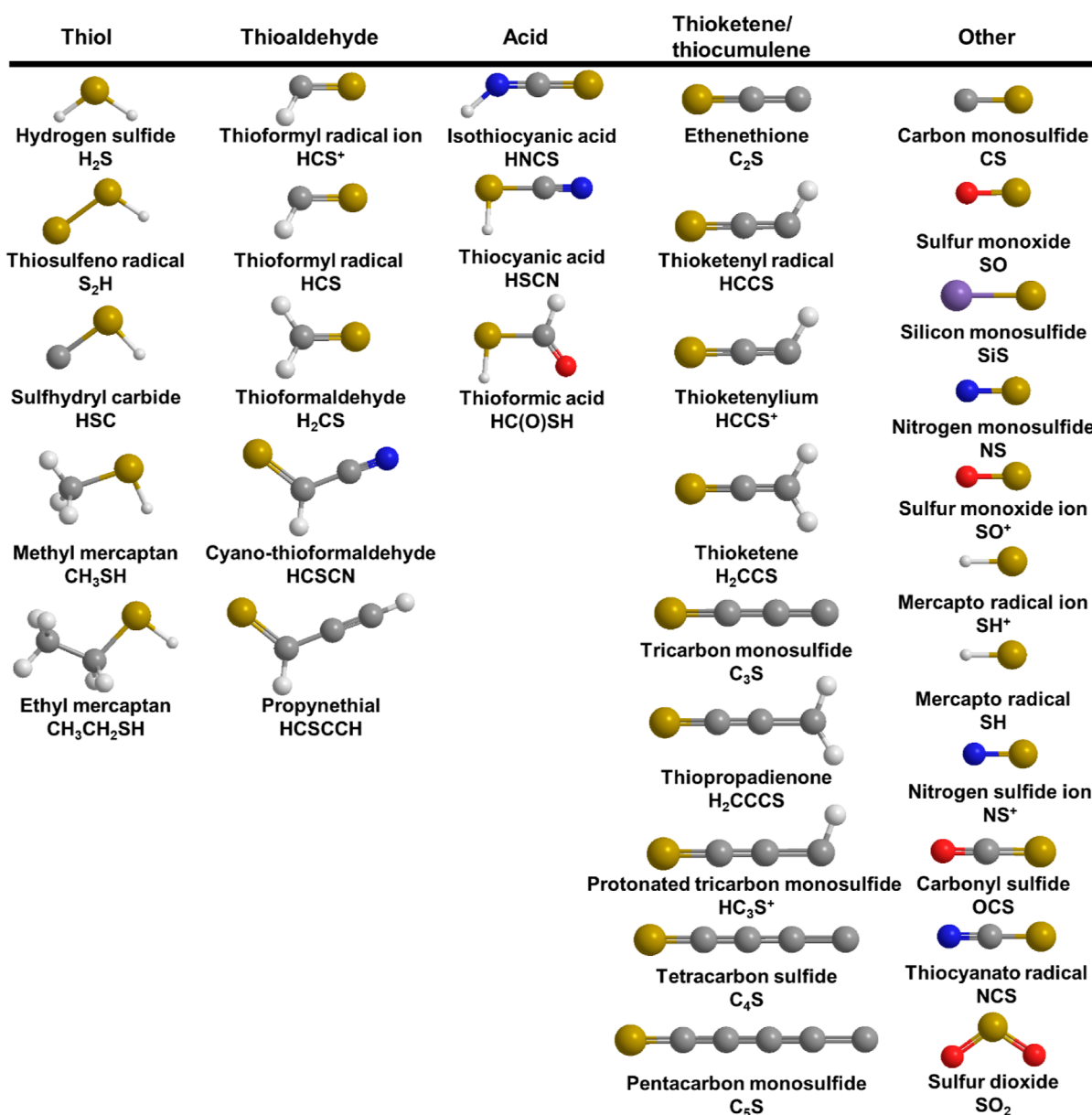


**Figure 1.** Key classes of sulfur-bearing molecules identified in the ISM. The colors correspond to the following elements: hydrogen (white), carbon (gray), nitrogen (blue), oxygen (red), sulfur (yellow), and silicon (purple).

expected theoretical equilibrium ratio.<sup>15</sup> They tentatively detected both conformers with abundances of  $(2.0 \pm 0.6) \times 10^{-9}$  and  $(5.4 \pm 1.8) \times 10^{-10}$  for *trans*- and *cis*-HCOSH, respectively, providing a *trans/cis* ratio of  $3.7 \pm 1.3$  for thioformic acid (1). Compared with observational results, García de la Concepción et al. found that the ratios of the rate constants for the forward (*cis* to *trans*) and backward (*trans* to *cis*) isomerizations in the gas phase are consistent with the *trans/cis* ratios measured toward both G+0.693–0.027 and G31.41+0.31 sources.<sup>15</sup>

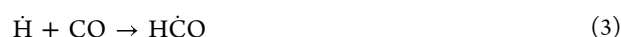
Several synthetic routes have been proposed for the formation mechanisms of thioformic acid (1) based on simple sulfur-bearing precursors. First, a possible pathway to the formation of thioformic acid (1) has been suggested to be reactions 1a and 1b.<sup>14</sup>



Alternatively, Molpeceres et al. theoretically characterized the hydrogenation channels of carbonyl sulfide (OCS) on the surface of amorphous solid water as an interstellar dust grain proxy in molecular clouds via reaction 1b.<sup>5,17</sup>



According to their calculations, reaction 2 may provide a possible pathway to *trans*-HCOSH, which explains the lower abundance of the *cis* conformer in astronomical observations.<sup>17</sup> Third, the radical–radical recombination pathway was proposed via reaction 4.<sup>14</sup>



The formyl radical ( $\dot{\text{H}}\text{CO}$ ) can be formed from CO and  $\dot{\text{H}}$  produced by energetic electron irradiation (reaction 3),<sup>18</sup> while

SH can be produced even within ices via radiolysis of hydrogen sulfide ( $\text{H}_2\text{S}$ ).

Here, we present surface-science experiments on the formation of thioformic acid (**1**)—the simplest thioacid—in low-temperature interstellar model ices composed of carbon monoxide and hydrogen sulfide. Binary ice ( $\text{CO}-\text{H}_2\text{S}$ ) mixtures were irradiated at temperatures as low as 5 K by energetic electrons, which were used to simulate secondary electrons generated in the track of galactic cosmic rays (GCRs) over typical lifetimes of molecular clouds of few million years.<sup>19</sup> Note that hydrogen sulfide-containing ices have received great attention in the context of interstellar and planetary surface science chemistry.<sup>7,10,20</sup> Until now, UV photolysis and proton exposure of ices containing hydrogen sulfide as the sulfur source and carbon monoxide as the carbon source have been studied and products such as hydrogen disulfide ( $\text{H}_2\text{S}_2$ ), formaldehyde ( $\text{H}_2\text{CO}$ ), OCS, and carbon disulfide ( $\text{CS}_2$ ) were formed.<sup>10,20–22</sup> To our knowledge, no study has examined the effect of electron irradiation on carbon monoxide (CO) hydrogen sulfide ( $\text{H}_2\text{S}$ ) ice mixtures. Exploiting the advantages of vacuum ultraviolet (VUV) photoionization reflectron time-of-flight mass spectrometry (PI-ReToF-MS) in the present experiments, the subliming products in the irradiated ices were detected in the gas phase via fragment-free isomer-specific photoionization during the temperature-programmed desorption (TPD), as the irradiated ices are heated from 5 K to 320 K.<sup>23</sup> The identification of thioformic acid (**1**) has important implications for the formation of prebiotic sulfur-bearing molecules, such as cysteine which may be a catalyst and precursor in the prebiotic synthesis of peptides.<sup>24,25</sup> Such molecules formed in the interstellar ices can be eventually incorporated into comets and may be delivered to planets such as Earth.<sup>26</sup> Therefore, our results further contribute to the understanding of the formation pathways of sulfur-bearing molecules detected in the ISM, shed light on the prebiotic synthesis of proteins,<sup>14</sup> and thus expand our knowledge on the evolution of biorelevant molecules in the universe.

## 2. METHODS

**2.1. Experimental.** The experiments were conducted in an ultrahigh vacuum (UHV) chamber evacuated to a few  $10^{-11}$  Torr.<sup>27</sup> Carbon monoxide (CO, Sigma-Aldrich, > 99%) and hydrogen sulfide ( $\text{H}_2\text{S}$ , Sigma-Aldrich, > 99.5%) were premixed in a separate chamber at a ratio of 2.5:1. The premixed gas was introduced to the main chamber at a pressure of  $4 \times 10^{-8}$  Torr via a glass capillary array and deposited onto a rhodium-coated silver substrate, which was mounted on an oxygen-free copper cold finger and cooled to 5 K by a closed-cycle helium refrigerator (Sumitomo Heavy Industries, RDK-415E). During deposition, the ice growth was monitored in situ via laser interferometry with a helium–neon laser (Melles Griot; 25-LHP-230) operating at 632.8 nm.<sup>28</sup> Considering the concentration-weighted average of  $1.32 \pm 0.12$  between the refractive indices of amorphous carbon monoxide ice ( $n = 1.25 \pm 0.03$ )<sup>29–31</sup> and hydrogen sulfide ( $n = 1.41 \pm 0.01$ ),<sup>32</sup> the ice thickness was determined to be  $720 \pm 90$  nm.<sup>28</sup> After deposition, the ices were irradiated with 5 keV electrons at a current of 20 nA for 10 min, resulting in a dose of up to 0.30 and 0.49 eV per molecule for carbon monoxide and hydrogen sulfide, respectively. For an interstellar ice grain, these doses are equivalent to few million years of exposure to galactic cosmic rays in the interior of a molecular cloud.<sup>19</sup> Using the

densities of carbon monoxide ( $0.8 \text{ g cm}^{-3}$ )<sup>29,31</sup> and hydrogen sulfide ( $1.1 \text{ g cm}^{-3}$ ),<sup>32,33</sup> the average electron penetration depth of the ice was calculated to be  $400 \pm 40$  nm according to Monte Carlo simulations carried out in the CASINO software suite.<sup>34</sup> This average depth was much less than the thicknesses of the ice, preventing electrons from reaching the substrate. Fourier transform infrared (FTIR) spectra were collected before, during, and after the irradiation to track changes in the chemical composition using the FTIR spectrometer (Thermo Nicolet 6700,  $4 \text{ cm}^{-1}$  resolution). The ratio of the CO:  $\text{H}_2\text{S}$  ices ( $1.7 \pm 0.3$ ):1 was determined by utilizing the bands and the absorption coefficients of  $2090 \text{ cm}^{-1}$  ( $\nu_1$ ,  $^{13}\text{CO}$ ,  $1.3 \times 10^{-17} \text{ cm molecule}^{-1}$ ),  $4249 \text{ cm}^{-1}$  ( $2\nu_1$ , CO,  $1.04 \times 10^{-19} \text{ cm molecule}^{-1}$ ), and  $2548 \text{ cm}^{-1}$  ( $\nu_3$ ,  $\text{H}_2\text{S}$ ,  $1.12 \times 10^{-17} \text{ cm molecule}^{-1}$ ).<sup>29,32,35</sup> After irradiation, the TPD scheme heated the ice from 5 to 320 K at a rate of  $1 \text{ K min}^{-1}$  to desorb the reactants and reaction products. During the TPD phase, the subliming species were photoionized, utilizing a pulsed VUV source, and the resulting ions were detected with a reflectron time-of-flight mass spectrometer (Jordan TOF Products, Inc.) equipped with two microchannel plates (MCPs) in a chevron geometry. Considering the computed ionization energy of thioformic acid (**1**, IE = 10.48–10.58 eV) (Table 1), photon energies at 10.82 and 10.39 eV were chosen to distinguish  $\text{CH}_2\text{SO}$  isomers based on their ionization energies (Figure 2). A 10.82 eV photon, if present, is capable of ionizing

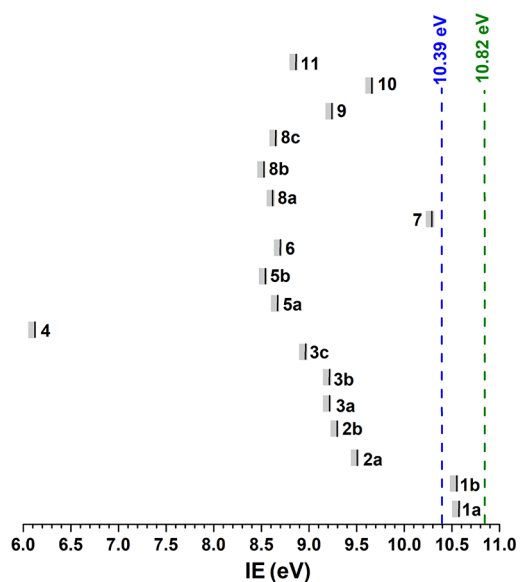


**Figure 2.** Computed ionization energies (IEs) of  $\text{CH}_2\text{SO}$  isomers (solid line) along with error limits (Table 1). The numbers 1 to 11 correspond to the isomers 1 to 11 in Table 1. Two vacuum ultraviolet (VUV) photon energies at 10.39 eV and 10.82 eV (dashed lines) were exploited in distinct experiments to ionize the subliming molecules during the TPD process.

all isomers; however, a 10.39 eV photon was chosen to ionize isomers 2–11 but not thioformic acid (**1**). The VUV photons (10.82 and 10.39 eV) were generated through resonant four-wave mixing (FWM) of two synchronized pulsed laser beams, which are produced by two dye lasers (Sirah, Cobra-Stretch) pumped by two Nd:YAG (neodymium-doped yttrium aluminum garnet) lasers (Spectra-Physics, Quanta Ray Pro 250–30 and 270–30, 30 Hz) (Table S1). The 10.82 eV (114.588 nm) photons were produced by difference FWM

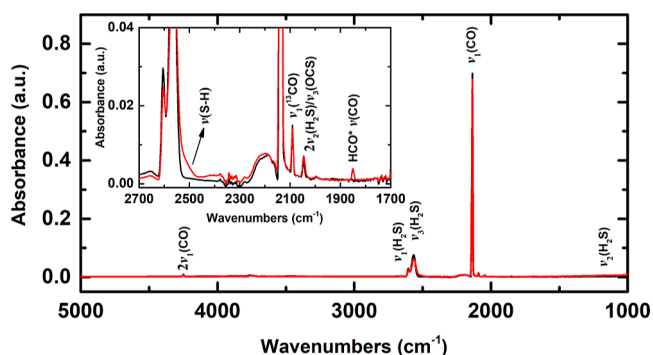


( $2\omega_1 - \omega_2$ ) in pulsed jets of krypton gas with  $\omega_1 = 202.316$  nm and  $\omega_2 = 863.117$  nm. An Nd:YAG laser pumped a Rhodamine 610/640 dye mixture to obtain 606.948 nm, producing  $\omega_1 = 202.316$  nm via third harmonic generation. A second Nd:YAG laser pumped LDS 867 dye to obtain  $\omega_2 = 863.117$  nm. To produce 10.39 eV (119.330 nm) light, difference FWM was performed in pulsed jets of krypton gas with  $\omega_1 = 202.316$  nm and  $\omega_2 = 664.271$  nm, which was generated from DCM (2-[2-[(E)-2-[4-(dimethylamino)phenyl]ethenyl]-6-methylpyran-4-ylidene]propanedinitrile) dye (in DMSO) pumped by Nd:YAG laser. The VUV photons were separated from photons with other energies using a biconvex lithium fluoride lens (Korth Kristalle GmbH) in an off-axis geometry and passed 2 mm above the silver substrate to ionize subliming molecules. The ion signals were amplified by a fast preamplifier (Ortec 9305) and recorded by a multichannel scaler (FAST ComTec, MCS6A). For each recorded mass spectra during the TPD phase, the accumulation time was 2 min (3600 sweeps) in 3.2 ns bin widths. The sublimed molecules during the TPD were also monitored by the electron impact quadrupole mass spectrometer (QMS; Extrel, model S221) operating at 70 eV and an emission current of 2 mA. An additional experiment without electron irradiation (blank) was performed at 10.82 eV to verify that the observed signals were produced by an external energy source. Isotopically labeled ices, such as  $C^{18}O-H_2S$  ( $C^{18}O$ , Sigma-Aldrich, 95 atom %  $^{18}O$ ) ice,  $^{13}CO-H_2S$  ( $^{13}CO$ , Sigma-Aldrich, < 5 atom %  $^{18}O$ , 90 atom %  $^{13}C$ ) ice, and  $CO-D_2S$  ( $D_2S$ , Sigma Aldrich, 97 atom % D) ice, were used to confirm the assigned species at the photon energy of 10.82 eV.

**2.2. Electronic Structure Calculations of Geometries and Ionization Energies.** All calculations are performed in the gas phase. The long-range corrected hybrid  $\omega B97XD$  density functional<sup>36</sup> with Dunning's correlation-consistent triple- $\zeta$  cc-pVTZ basis set<sup>37</sup> was used for the geometry optimization of the variety of neutral  $CH_2SO$  isomers and their cations. The same  $\omega B97XD/cc-pVTZ$  method was employed to compute their vibrational frequencies and zero-point vibrational energy corrections (ZPE). Then, coupled-cluster theory was applied to refine single-point energies using the optimized  $\omega B97XD/cc-pVTZ$  geometries of the neutral and cationic molecules and to assess relative energies and adiabatic ionization energies (AIE) of the neutral  $CH_2SO$  species. In particular, we utilized the explicitly correlated RCCSD(T)-F12b method<sup>38</sup> including single and double excitations with the perturbative treatment of triple excitations with Dunning's quadruple- $\zeta$  cc-pVQZ-F12 basis set. The anticipated accuracy of the CCSD(T)-F12b/cc-pVQZ-F12// $\omega B97XD/cc-pVTZ + ZPE(\omega B97XD/cc-pVTZ)$  computational scheme is within 0.01–0.02 Å for bond lengths, 1–2° for bond angles, and about 0.04 eV for AIE.<sup>39</sup> The electronic structure calculations were carried out employing the Gaussian 16<sup>40</sup> and MOLPRO 2021 packages<sup>41</sup> for  $\omega B97XD$  and CCSD(T)-F12b, respectively. Note that the ionization energies of the subliming molecules decrease by up to 0.03 eV due to the static-electric-field-induced Stark shift.<sup>27</sup> Based on the electrical effect of –0.03 eV and computed IE error of  $\pm 0.04$  eV, the error analyses of computed ionization energies of  $CH_2SO$  isomers are listed in Table 1. Furthermore, Table S3 shows the optimized molecular coordinates and calculated harmonic vibrational frequencies.

### 3. RESULTS AND DISCUSSION

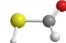
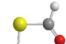
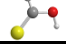
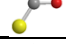
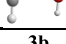


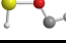
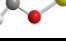
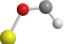
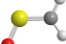
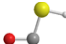
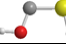


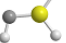
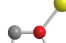
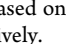
**3.1. IR Spectroscopy.** IR spectroscopy represents an elegant tool for the identification of small molecules along with functional groups of complex organics during the irradiation process of ices.<sup>23</sup> The FTIR spectra of the carbon monoxide (CO)hydrogen sulfide ( $H_2S$ ) ice mixture before (black) and after (red) irradiation along with assignments are shown in Figure 3. All absorptions in the IR spectrum taken before



**Figure 3.** IR spectrum of pristine (black) and irradiated (red) carbon monoxide (CO) hydrogen sulfide ( $H_2S$ ) ice at 5 K. Detailed assignments are compiled in Table S2. Inset: zoomed region from 2700 to 1700  $cm^{-1}$ , revealing new peaks after irradiation.

irradiation can be associated with carbon monoxide and hydrogen sulfide, such as the CO stretch ( $\nu_1$ , 2136  $cm^{-1}$ ) of carbon monoxide<sup>42</sup> and S–H stretching modes ( $\nu_1$ , 2603  $cm^{-1}$ ;  $\nu_3$ , 2566  $cm^{-1}$ ) of hydrogen sulfide.<sup>7,13,20</sup> After irradiation, several new absorptions emerged in the 2700–1700  $cm^{-1}$  region (red line in Figure 3). The difference IR spectrum between the irradiated and pristine CO– $H_2S$  ice is shown in Figure S1. Table S2 summarizes the IR absorption features of the pristine ice and new absorption features after irradiation. The formyl radical (HCO) is identified from the  $\nu_3$  fundamental (CO stretch) at 1840  $cm^{-1}$  in irradiated ices.<sup>26,42</sup> The feature at 2045  $cm^{-1}$  was present prior to the irradiation and was assigned to the overtone mode ( $2\nu_2$ ) of hydrogen sulfide; however, this peak increased after irradiation, suggesting that it is also associated with the formed products. Ferrante et al. reported the absorption features of OCS ( $\nu_3$ ) at 2047 and 2054  $cm^{-1}$  in CO–OCS ice and  $CO_2$ –OCS ice at 11 K, respectively.<sup>21</sup> Therefore, this absorption feature can be assigned to OCS, which was formed in both UV photolysis and proton radiolysis of CO– $H_2S$  ice.<sup>10,20–22</sup> As absorption features for S–H stretching of sulfur-containing molecules are located in the 2650–2400  $cm^{-1}$  region,<sup>20</sup> the new absorption feature at 2518  $cm^{-1}$  could be associated with S–H stretching of sulfur-containing products such as  $H_2S_n$  ( $n \geq 2$ ). Based on the computed anharmonic vibrational spectrum of thioformic acid,<sup>43</sup> no absorption peaks from thioformic acid were observed after irradiation (Figure 3). It should be noted that our experimental conditions with low-dose irradiation (20 nA, 10 min) are selected to obtain mechanistic information which requires an investigation of the initial reaction steps. Since FTIR spectroscopy in the case of complex mixtures primarily identifies only functional groups of organic molecules, the newly formed molecules cannot be uniquely assigned and therefore, an additional experimental technique is required to probe discrete reaction products.

Table 1. Error Analysis of Computed Ionization Energies of CH<sub>2</sub>SO Isomers; Adiabatic Ionization Energies (IE) and Relative Energies  $E_{\text{rel}}$  Were Computed at the CCSD(T)-F12/cc-pVQZ-F12// $\omega$ B97XD/cc-pVTZ + ZPE( $\omega$ B97XD/cc-pVTZ) Level of Theory<sup>a</sup>

Isomer	$E_{\text{rel}}$ (kJ mol <sup>-1</sup> )	Computed IE (eV)	Computed IE range (eV)	IE range (eV)
<b>1a</b> 	3	10.57	10.53 – 10.61	10.50 – 10.58
<b>1b</b> 	0	10.55	10.51 – 10.59	10.48 – 10.56
<b>2a</b> 	14	9.55	9.51 – 9.59	9.48 – 9.56
<b>2b</b> 	35	9.30	9.26 – 9.34	9.23 – 9.31
<b>3a</b> 	221	9.21	9.17 – 9.25	9.14 – 9.22
<b>3b</b> 	219	9.21	9.17 – 9.25	9.14 – 9.22
<b>3c</b> 	242	8.95	8.91 – 8.99	8.88 – 8.96
<b>4</b> 	404	6.12	6.08 – 6.16	6.05 – 6.13
<b>5a</b> 	351	8.67	8.63 – 8.71	8.60 – 8.68
<b>5b</b> 	355	8.54	8.50 – 8.58	8.47 – 8.55
<b>6</b> 	259	8.70	8.66 – 8.74	8.63 – 8.71
<b>7</b> 	93	10.29	10.25 – 10.33	10.22 – 10.30
<b>8a</b> 	180	8.52	8.48 – 8.56	8.45 – 8.53
<b>8b</b> 	181	8.61	8.57 – 8.65	8.54 – 8.62
<b>8c</b> 	196	8.65	8.61 – 8.69	8.58 – 8.66
<b>9</b> 	164	9.22	9.18 – 9.26	9.15 – 9.23
<b>10</b> 	379	9.65	9.61 – 9.69	9.58 – 9.66
<b>11</b> 	571	8.86	8.82 – 8.90	8.79 – 8.87

<sup>a</sup>The IE ranges are calculated based on the electrical effect of  $-0.03$  eV and computed IE error of  $\pm 0.04$  eV. The isomers **1a** and **1b** correspond to *cis*- and *trans*-HCOSH, respectively.

**3.2. PI-ReToF-MS.** PI-ReToF-MS is exploited to understand the formation pathways of complex organic molecules (COMs) within interstellar analogue ices.<sup>23,44</sup> This technique

is utilized here to identify individual CH<sub>2</sub>SO isomers formed in irradiated CO–H<sub>2</sub>S ice based on their ionization energies. The PI-ReToF-MS data of the photoionized, desorbing molecules

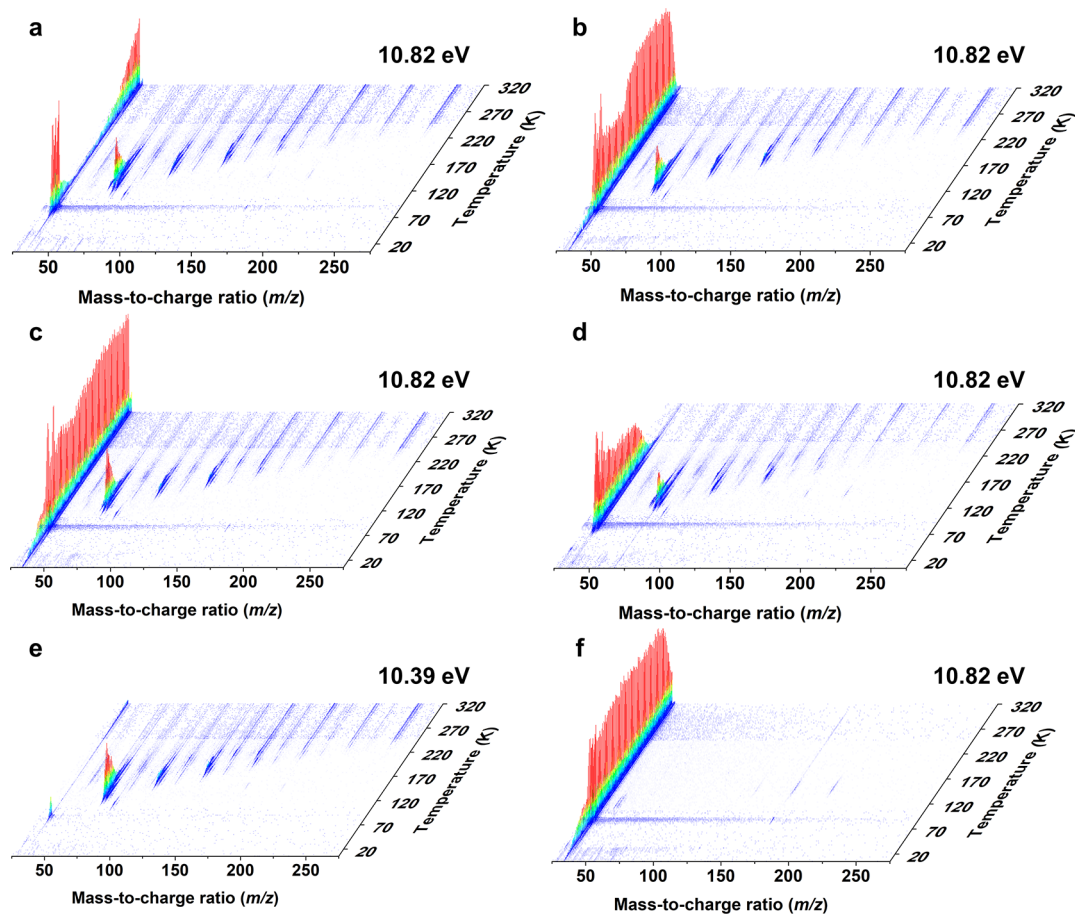


**Figure 4.** PI-ReToF-MS spectra collected during the TPD phase of the subliming carbon monoxide–hydrogen sulfide ices: (a,e) from CO–H<sub>2</sub>S ice photoionized at (a) 10.82 and (e) 10.39 eV, (b) from C<sup>18</sup>O–H<sub>2</sub>S ice photoionized at 10.82 eV, (c) from <sup>13</sup>CO–H<sub>2</sub>S ice photoionized at 10.82 eV, and (d) from CO–D<sub>2</sub>S ice photoionized at 10.82 eV. (f) Blank experiment of the CO–H<sub>2</sub>S ice (10.82 eV).

from the irradiated ices are compiled in Figure 4; these raw data are required to extract TPD profiles of  $m/z = 62$  at two photon energies of 10.82 and 10.39 eV (Figure 5a). The TPD profile at  $m/z = 62$  recorded at a photon energy of 10.82 eV reveals two distinct sublimation events. The first event has a peak sublimation temperature at 89 K in both irradiated and unirradiated (blank experiment) ices. The desorption of H<sub>2</sub>S ices peaks at 86 K (Figure S2); this weak sublimation event is due to saturation of the detector upon sublimation of H<sub>2</sub>S (IE =  $10.453 \pm 0.008$  eV). The second, strong sublimation event starts at 116 K, peaks around 131 K, and returns to baseline level at 225 K. It should be noted that these ion counts are not present in the blank experiments, that is, in experiments conducted with subliming unirradiated CO–H<sub>2</sub>S ice at a photon energy of 10.82 eV (Figure 5a). Given the molecular weights of the reactants,  $m/z = 62$  could belong to the formula for CH<sub>2</sub>O<sub>3</sub>, CH<sub>2</sub>SO, C<sub>2</sub>H<sub>6</sub>S, C<sub>2</sub>H<sub>6</sub>O<sub>2</sub>, and C<sub>3</sub>H<sub>2</sub>. By matching the TPD profiles for the isotopically labeled molecules in irradiated C<sup>18</sup>O–H<sub>2</sub>S ice (CH<sub>2</sub>S<sup>18</sup>O<sup>+</sup>,  $m/z = 64$ ), <sup>13</sup>CO–H<sub>2</sub>S ice (<sup>13</sup>CH<sub>2</sub>SO<sup>+</sup>,  $m/z = 63$ ), and CO–D<sub>2</sub>S ice (CD<sub>2</sub>SO<sup>+</sup>,  $m/z = 64$ ) (Figure 5b), the assignment of this signal peaking at about 131 K can be clearly linked to the CH<sub>2</sub>SO isomers. In particular, the replacement of the CO–H<sub>2</sub>S ice by <sup>13</sup>CO–H<sub>2</sub>S ice shifts the  $m/z$  by 1 amu from  $m/z = 62$  to 63, indicating the presence of a single carbon atom. Furthermore, the shift by 2 amu from  $m/z = 62$  to 64 in the C<sup>18</sup>O–H<sub>2</sub>S and CO–D<sub>2</sub>S ices indicates the presence of one oxygen atom and of two

deuterium atoms, respectively. Therefore, the sublimation event peaking at about 131 K can be clearly linked to a molecule of the formula CH<sub>2</sub>SO. Note that the sublimation events peaking at 161 K for  $m/z = 64$  in the C<sup>18</sup>O–H<sub>2</sub>S or CO–D<sub>2</sub>S ice originates from the S<sub>2</sub><sup>+</sup> photofragment of H<sub>2</sub>S<sub>3</sub> ( $m/z = 98$ ) or D<sub>2</sub>S<sub>3</sub> ( $m/z = 100$ ), respectively (Figure S3). The formula H<sub>2</sub>S<sub>3</sub> for the ion signal at  $m/z = 98$  was confirmed based on the results of isotopically labeled experiments (Figure S3).

Having identified the molecular formula of the molecule subliming at about 131 K as CH<sub>2</sub>SO, we are now distinguishing thioformic acid (1) from the other remaining CH<sub>2</sub>SO isomers. This requires carrying out experiments at photon energies of 10.82 and 10.39 eV as indicated in Figure 2. The ionization energies for all possible CH<sub>2</sub>SO isomers were calculated (Table 1). At 10.82 eV, all CH<sub>2</sub>SO isomers can be photoionized. Therefore, at 10.82 eV, the second sublimation event peaking at 131 K in the irradiated CO–H<sub>2</sub>S ice at  $m/z = 62$  (Figures 5a) can be associated with any isomer from 1–11 (IE = 6.05–10.58 eV). The experiment at a photon energy of 10.39 eV can only ionize—if present—isomers 2–11 (IE = 6.05–10.30 eV), but not thioformic acid (1). No ions were observed in irradiated CO–H<sub>2</sub>S ice at  $m/z = 62$  (Figures 5a), eliminating isomers 2–11 as potential products. Thus, the sublimation event peaking at 131 K at 10.82 eV is connected solely to thioformic acid (1).

Note that the two most abundant sulfur isotopes are  $^{32}\text{S}$  and  $^{34}\text{S}$  with natural abundances of 95.02 and 4.21%, respectively.

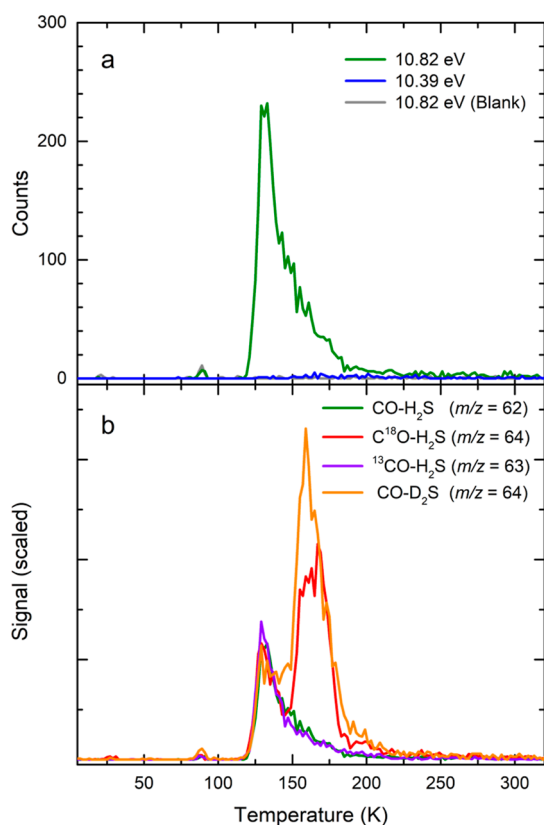


**Figure 5.** (a) TPD profiles for  $\text{CH}_2^{32}\text{SO}$  ( $m/z = 62$ ) from the irradiated  $\text{CO-H}_2\text{S}$  ice at 10.82 eV (red), 10.39 eV (blue), and in unirradiated (blank)  $\text{CO-H}_2\text{S}$  ice at 10.82 eV (gray). (b) TPD profiles at 10.82 eV for isotopically labeled  $\text{CO-H}_2\text{S}$  ice mixtures.

**Figure 6** shows the TPD profiles for different isotopologues of thioformic acid (**1**) collected at 10.82 eV in  $\text{CO-H}_2\text{S}$  ice ( $\text{HCO}^{32}\text{SH}$  and  $\text{HCO}^{34}\text{SH}$ ),  $\text{C}^{18}\text{O-H}_2\text{S}$  ice ( $\text{HC}^{18}\text{O}^{32}\text{SH}$  and  $\text{HC}^{18}\text{O}^{34}\text{SH}$ ),  $^{13}\text{CO-H}_2\text{S}$  ice ( $\text{H}^{13}\text{CO}^{32}\text{SH}$  and  $\text{H}^{13}\text{CO}^{34}\text{SH}$ ), and  $\text{CO-D}_2\text{S}$  ice ( $\text{DCO}^{32}\text{SD}$  and  $\text{DCO}^{34}\text{SD}$ ). The dashed

lines indicate the sublimation peak of thioformic acid (**1**). In the irradiated  $\text{CO-H}_2\text{S}$  ice, the sublimation event peaking at 131 K at  $m/z = 62$  corresponds to the  $\text{HCO}^{32}\text{SH}$  and comprises  $3020 \pm 300$  ion counts. The TPD profile at  $m/z = 64$  in  $\text{CO-H}_2\text{S}$  ice reveals three distinct sublimation events (**Figure 5a**). It should be noted that the first sublimation event peaking at 89 K results from the saturation of the  $\text{H}_2\text{S}$  signal. The third event, peaking at 162 K at  $m/z = 64$ , corresponds to the  $\text{S}_2^+$  fragment. The second event has  $145 \pm 15$  ion counts and an intensity of  $4.8 \pm 0.7\%$  compared to  $\text{HCO}^{32}\text{SH}$  at  $m/z = 62$ , with a peak sublimation temperature at 131 K. Likewise, a similar fraction of  $4.9 \pm 0.7\%$  is obtained in  $^{13}\text{CO-H}_2\text{S}$  ice (**Figure 5c**). These two ratios match the natural abundance ratio of about 4.5% of  $^{32}\text{S}:^{34}\text{S}$ , suggesting that the sublimation events peaking at 131 K in **Figures 5a,c** are linked to  $\text{HCO}^{34}\text{SH}$  and  $\text{H}^{13}\text{CO}^{34}\text{SH}$ , respectively. The sublimation events that peak at 128 K at  $m/z = 66$  in  $\text{C}^{18}\text{O-H}_2\text{S}$  ice (**Figure 5b**) or  $\text{C}^{18}\text{O-D}_2\text{S}$  ice (**Figure 5d**) are associated with  $\text{H}_2\text{S}_2^+$  and  $\text{HC}^{18}\text{O}^{34}\text{SH}$  or  $\text{DCO}^{34}\text{SD}$ .

Having provided compelling evidence for the synthesis of thioformic acid (**1**) in interstellar ice analogues, we shift our attention to the formation pathways. It is important to note that there have been extensive studies on  $\text{CO-H}_2\text{O}$  ice analogues under simulated astrophysical conditions, which involve reactions initiated by VUV photolysis,<sup>45</sup> protons (0.8 MeV),<sup>46</sup> electrons (5 keV),<sup>47–49</sup> X-rays,<sup>50</sup> and energetic heavy ions (46 MeV  $^{58}\text{Ni}^{11+}$ ).<sup>51</sup> These results reported the production of formyl radical ( $\text{HCO}$ ) and formic acid ( $\text{HCOOH}$ ), which is one of the most abundant products. The IR spectroscopy and isotopic substitution results showed that the hydrogen atom and hydroxyl radical from  $\text{H}_2\text{O}$  can add to  $\text{CO}$  to form  $\text{HCO}$  and  $\text{HCOOH}$ .<sup>46</sup> The astrochemical pathways for thioformic acid (**1**) could be similar to the formation of  $\text{HCOOH}$  in the processed  $\text{CO-H}_2\text{O}$  ice.<sup>14</sup> Therefore, we propose the potential reaction mechanism for its formation in **Figure 7**. First, the path toward thioformic acid (**1**) begins with hydrogen sulfide molecule being radiolyzed to a mercapto radical ( $\text{SH}$ ) plus a hydrogen atom (reaction (S));<sup>7,13</sup> this process is endoergic by  $378 \text{ kJ mol}^{-1}$  and can be supplied by the impinging GCR proxy. Second, the addition of a hydrogen atom to carbon monoxide leads to the formation of

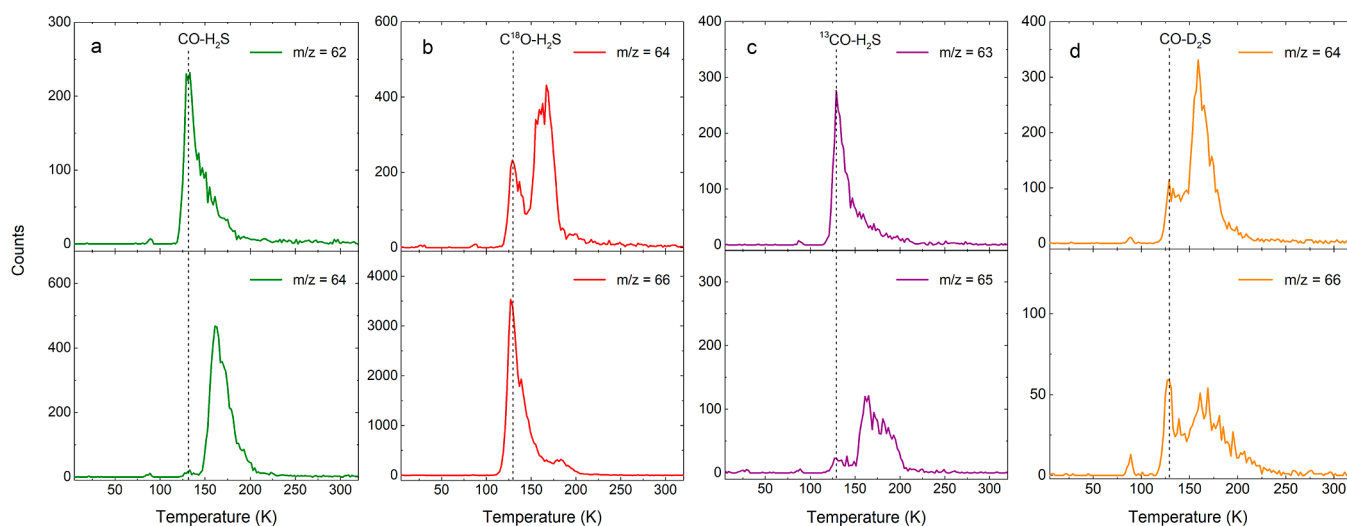


**Figure 6.** TPD profiles for different isotopologues of thioformic acid (**1**,  $\text{HC(O)SH}$ ) recorded at 10.82 eV in  $\text{CO-H}_2\text{S}$  ice (a),  $\text{C}^{18}\text{O-H}_2\text{S}$  ice (b),  $^{13}\text{CO-H}_2\text{S}$  ice (c), and  $\text{CO-D}_2\text{S}$  ice (d). The dashed line indicates the sublimation peak of thioformic acid (**1**).



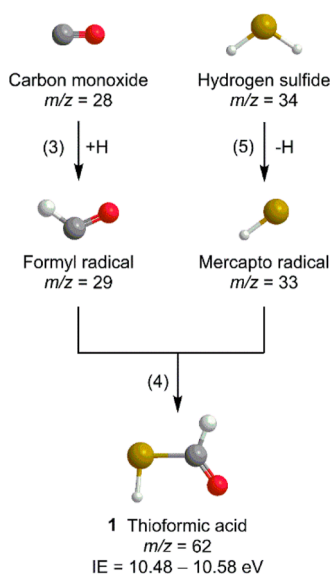


**Figure 7.** Reaction pathways from carbon monoxide and hydrogen sulfide leading to thioformic acid (1) determined by PI-ReToF-MS.

formyl radical ( $\dot{\text{H}}\text{CO}$ ) via reaction (3) as detected via FTIR (Table S2). The entrance barrier for this reaction is 11  $\text{kJ mol}^{-1}$ , while the overall formation of the formyl radical is exoergic by 60  $\text{kJ mol}^{-1}$ .<sup>52</sup> Note that the entrance barrier of 11  $\text{kJ mol}^{-1}$  could be overcome by the energy contributed by GCRs. The barrierless radical–radical recombination of formyl radical ( $\dot{\text{H}}\text{CO}$ ) and mercapto radical ( $\dot{\text{S}}\text{H}$ ) leads to the formation of thioformic acid (1) via reaction (4). Note that no evidence was observed for the formation of ionic species in the FTIR spectra after irradiation (Figure 3); the role of ions involved in the formation of thioformic acid (1) has not been considered. Overall, the reaction of hydrogen sulfide with carbon monoxide to form thioformic acid (1) is endoergic by 10  $\text{kJ mol}^{-1}$ , thus highlighting the critical role of irradiation-stimulated chemistry in the formation of thioformic acid (1).



Carbon monoxide is the second most abundant molecule on icy grains and has been detected at levels up to 50% relative to water in the interstellar medium toward the envelope around the intermediate-mass class I Young Stellar Objects (YSOs).<sup>53</sup> Suggested to be formed by hydrogenation on dust grains,<sup>54</sup> hydrogen sulfide has an abundance in the range of  $10^{-10}$ – $10^{-6}$  relative to molecular hydrogen.<sup>55</sup> Both carbon monoxide and hydrogen sulfide are present in hot core G31.41+0.31<sup>56,57</sup> and the G+0.693 molecular cloud.<sup>58,59</sup> The molecular gases in G+0.693 are located in the Galactic Center and are affected by an enhanced cosmic ray ionization rate (CRIR), which is 2–3 orders of magnitude higher than that of the standard CRIR.<sup>60</sup> It is important to note that thioformic acid (1) was detected toward the giant molecular cloud G+0.693–0.027 recently;<sup>14</sup> therefore, our findings may be particularly relevant for the formation of thioformic acid (1) toward G+0.693. Through radical recombination reactions of the formyl radical ( $\dot{\text{H}}\text{CO}$ ) with the mercapto radical ( $\dot{\text{S}}\text{H}$ ) within interstellar ices, carbon monoxide and hydrogen sulfide could represent critical precursors for the formation of thioformic acid (1). After formation, thioformic acid (1) may react with other adsorbed species on the grains and produce other organo-sulfur molecules, contributing to interstellar sulfur depletion.

## 4. CONCLUSIONS

To conclude, our results present the first formation of thioformic acid (1) in laboratory interstellar ice analogues composed of carbon monoxide (CO) and hydrogen sulfide ( $\text{H}_2\text{S}$ ), providing crucial information on the formation of thioformic acid (1) in interstellar space. Thioformic acid (1) was detected in the gas phase during the TPD phase with a sublimation peak at 131 K at 10.82 eV. Alternative  $\text{CH}_2\text{SO}$  isomers were ruled out as contributors to the signal by lowering the photon energy to 10.39 eV. Recent work by Nguyen et al. identified the formation of thioformic acid based on the IR spectrum of the products in the reaction of solid OCS with hydrogen atoms on amorphous solid water.<sup>5</sup> However, earlier studies<sup>10,20–22</sup> did not identify thioformic acid (1) in sulfur-containing systems, such as CO– $\text{H}_2\text{S}$  ice, via IR spectroscopy and/or mass spectrometry utilizing electron impact ionization, possibly due to the small amount in the product<sup>5</sup> and the overlap of the fundamentals of thioformic acid (1) with precursor molecules. Therefore, our results demonstrate the unique power of PI-ReToF-MS to identify complex sulfur-containing molecules in space simulation experiments. Thioacids have been proposed as one of the key agents in the prebiotic polymerization of amino acids into peptides and proteins;<sup>14,24</sup> therefore, our findings shed light on the prebiotic synthesis of biorelevant molecules in deep space. Since water is the main constituent of ice in realistic interstellar conditions, future experiments incorporating water into the ice mixture may unravel the formation mechanisms of more organosulfur species, such as hydrogen thioperoxide (HSOH), and thus may help clarify the sulfur depletion problem.<sup>5</sup>

## ■ ASSOCIATED CONTENT

### Supporting Information

The Supporting Information is available free of charge at <https://pubs.acs.org/doi/10.1021/acs.jpca.2c06860>.

Difference IR spectrum between the irradiated and pristine ice; QMS ion signals of reactants; TPD profiles for  $\text{S}_2^+$ ,  $\text{H}_2\text{S}_3^+$ , and  $\text{D}_2\text{S}_3^+$ ; parameters for the generation of VUV light; absorption peaks observed in CO– $\text{H}_2\text{S}$  ice; and Cartesian coordinates and vibrational frequencies of  $\text{CH}_2\text{SO}$  molecules (PDF)

## ■ AUTHOR INFORMATION

### Corresponding Author

Ralf I. Kaiser – Department of Chemistry and W. M. Keck Research Laboratory in Astrochemistry, University of Hawai'i at Manoa, Honolulu, Hawaii 96822, United States; [orcid.org/0000-0002-7233-7206](https://orcid.org/0000-0002-7233-7206); Email: [ralfk@hawaii.edu](mailto:ralfk@hawaii.edu)

### Authors

Jia Wang – Department of Chemistry and W. M. Keck Research Laboratory in Astrochemistry, University of Hawai'i at Manoa, Honolulu, Hawaii 96822, United States

Joshua H. Marks – Department of Chemistry and W. M. Keck Research Laboratory in Astrochemistry, University of Hawai'i at Manoa, Honolulu, Hawaii 96822, United States

Lotefa B. Tuli – Department of Chemistry and Biochemistry, Florida International University, Miami, Florida 33199, United States

Alexander M. Mebel – Department of Chemistry and Biochemistry, Florida International University, Miami,



Florida 33199, United States; [orcid.org/0000-0002-7233-3133](https://orcid.org/0000-0002-7233-3133)

Valeriy N. Azyazov – Lebedev Physical Institute, Samara 443011, Russia

Complete contact information is available at:  
<https://pubs.acs.org/10.1021/acs.jpca.2c06860>

### Author Contributions

<sup>#</sup>These authors contributed equally to this work.

### Notes

The authors declare no competing financial interest.

## ACKNOWLEDGMENTS

The Hawaii group acknowledges support from the US National Science Foundation, Division of Astronomical Sciences under grants AST-2103269 awarded to the University of Hawaii at Manoa. The ab initio calculations at Lebedev Physics Institute were supported by the Ministry of Science and Higher Education of the Russian Federation under grant no. 075-15-2021–597.

## REFERENCES

- (1) Penzias, A. A.; Solomon, P. M.; Wilson, R. W.; Jefferts, K. B. Interstellar Carbon Monosulfide. *Astrophys. J.* **1971**, *168*, L53.
- (2) Mifsud, D. V.; Kaňuchová, Z.; Herczku, P.; Ioppolo, S.; Juhász, Z.; Kovács, S. T. S.; Mason, N. J.; McCullough, R. W.; Sulik, B. Sulfur Ice Astrochemistry: A Review of Laboratory Studies. *Space Sci. Rev.* **2021**, *217*, 14.
- (3) Woon, D. E. The Astrochemist, 2021. (accessed 20 July, 2022) <http://www.astrochemist.org/>.
- (4) Le Gal, R.; Öberg, K. I.; Loomis, R. A.; Pegues, J.; Bergner, J. B. Sulfur Chemistry in Protoplanetary Disks: CS and H<sub>2</sub>CS. *Astrophys. J.* **2019**, *876*, 72.
- (5) Nguyen, T.; Oba, Y.; Sameera, W. M. C.; Kouchi, A.; Watanabe, N. Successive H-atom Addition to Solid OCS on Compact Amorphous Solid Water. *Astrophys. J.* **2021**, *922*, 146.
- (6) Oba, Y.; Tomaru, T.; Lamberts, T.; Kouchi, A.; Watanabe, N. An Infrared Measurement of Chemical Desorption from Interstellar Ice Analogues. *Nat. Astron.* **2018**, *2*, 228–232.
- (7) Jiménez-Escobar, A.; Muñoz Caro, G. M. Sulfur Depletion in Dense Clouds and Circumstellar Regions. *Astron. Astrophys.* **2011**, *536*, A91.
- (8) Kaňuchová, Z.; Boduch, P.; Domaracka, A.; Palumbo, M. E.; Rothard, H.; Strazzulla, G. Thermal and Energetic Processing of Astrophysical Ice Analogues Rich in SO<sub>2</sub>. *Astron. Astrophys.* **2017**, *604*, A68.
- (9) Garozzo, M.; Fulvio, D.; Gomis, O.; Palumbo, M. E.; Strazzulla, G. H-implantation in SO<sub>2</sub> and CO<sub>2</sub> Ices. *Planet. Space Sci.* **2008**, *56*, 1300–1308.
- (10) Chen, Y. J.; Juang, K. J.; Nuevo, M.; Jiménez-Escobar, A.; Muñoz Caro, G. M.; Qiu, J. M.; Chu, C. C.; Yih, T. S.; Wu, C. Y. R.; Fung, H. S.; et al. Formation of S-bearing Species by VUV/EUV Irradiation of H<sub>2</sub>S-containing Ice Mixtures: Photon Energy and Carbon Source Effects. *Astrophys. J.* **2015**, *798*, 80.
- (11) Carrier, W.; Jamieson, C. S.; Kaiser, R. I. Mechanistic Studies on the Formation of Trifluoromethyl Sulfur Pentafluoride, SF<sub>5</sub>CF<sub>3</sub> – a Greenhouse Gas. *Inorg. Chem.* **2007**, *46*, 1332–1336.
- (12) Goettl, S. J.; Doddipatla, S.; Yang, Z.; He, C.; Kaiser, R. I.; Silva, M. X.; Galvão, B. R. L.; Millar, T. J. Chemical Dynamics Study on the Gas-phase Reaction of the D1-silyldiyne Radical (SiD; X<sup>2</sup>Π) with Deuterium Sulfide (D<sub>2</sub>S) and Hydrogen Sulfide (H<sub>2</sub>S). *Phys. Chem. Chem. Phys.* **2021**, *23*, 13647–13661.
- (13) Cazaux, S.; Carrascosa, H.; Muñoz Caro, G. M.; Caselli, P.; Fuente, A.; Navarro-Almáida, D.; Riviére-Marichalar, P. Photo-processing of H<sub>2</sub>S on Dust Grains. *Astron. Astrophys.* **2022**, *657*, A100.
- (14) Rodríguez-Almeida, L. F.; Jiménez-Serra, I.; Rivilla, V. M.; Martín-Pintado, J.; Zeng, S.; Tercero, B.; de Vicente, P.; Colzi, L.; Rico-Villas, F.; Martín, S.; et al. Thiols in the Interstellar Medium: First Detection of HC(O)SH and Confirmation of C<sub>2</sub>H<sub>3</sub>SH. *Astrophys. J. Lett.* **2021**, *912*, L11.
- (15) García de la Concepción, J.; Colzi, L.; Jiménez-Serra, I.; Molpeceres, G.; Corchado, J. C.; Rivilla, V. M.; Martín-Pintado, J.; Beltrán, M. T.; Mininni, C. The trans/cis Ratio of Formic (HCOOH) and Thioformic (HC(O)SH) Acids in the Interstellar Medium. *Astron. Astrophys.* **2022**, *658*, A150.
- (16) Védova, C. O. D. Conformational Study of Monothioformic Acid, HC(O)SH. *J. Raman Spectrosc.* **1991**, *22*, 291–295.
- (17) Molpeceres, G.; García de la Concepción, J.; Jiménez-Serra, I. Diastereoselective Formation of Trans-HC(O)SH through Hydrogenation of OCS on Interstellar Dust Grains. *Astrophys. J.* **2021**, *923*, 159.
- (18) Bennett, C. J.; Jamieson, C. S.; Kaiser, R. I. Mechanical Studies on the Formation and Destruction of Carbon Monoxide (CO), Carbon dioxide (CO<sub>2</sub>), and Carbon Trioxide (CO<sub>3</sub>) in Interstellar Ice Analog Samples. *Phys. Chem. Chem. Phys.* **2010**, *12*, 4032–4050.
- (19) Yeghikyan, A. G. Irradiation of Dust in Molecular Clouds. II. Doses Produced by Cosmic rays. *Astrophysics* **2011**, *54*, 87–99.
- (20) Jiménez-Escobar, A.; Muñoz Caro, G. M.; Chen, Y.-J. Sulphur Depletion in Dense Clouds and Circumstellar Regions. Organic Products Made from UV Photoprocessing of Realistic Ice Analogs Containing H<sub>2</sub>S. *Mon. Not. R. Astron. Soc.* **2014**, *443*, 343–354.
- (21) Ferrante, R. F.; Moore, M. H.; Spiliotis, M. M.; Hudson, R. L. Formation of Interstellar OCS: Radiation Chemistry and IR Spectra of Precursor Ices. *Astrophys. J.* **2008**, *684*, 1210–1220.
- (22) Garozzo, M.; Fulvio, D.; Kanuchova, Z.; Palumbo, M. E.; Strazzulla, G. The Fate of S-bearing Species after Ion Irradiation of Interstellar Icy Grain Mantles. *Astron. Astrophys.* **2010**, *509*, A67.
- (23) Turner, A. M.; Kaiser, R. I. Exploiting Photoionization Reflectron Time-of-Flight Mass Spectrometry to Explore Molecular Mass Growth Processes to Complex Organic Molecules in Interstellar and Solar System Ice Analogs. *Acc. Chem. Res.* **2020**, *53*, 2791–2805.
- (24) Foden, C. S.; Islam, S.; Fernández-García, C.; Maugeri, L.; Sheppard, T. D.; Powner, M. W. Prebiotic Synthesis of Cysteine Peptides that Catalyze Peptide Ligation in Neutral Water. *Science* **2020**, *370*, 865–869.
- (25) Purzycka, J.; Custer, T.; Gronowski, M. UV Photolysis of C<sub>2</sub>H<sub>3</sub>SH in Solid CO and Ar. *ACS Earth Space Chem.* **2022**, *6*, 131–143.
- (26) Kleimeier, N. F.; Kaiser, R. I. Bottom-Up Synthesis of 1,1-Ethenediol (H<sub>2</sub>CC(OH)<sub>2</sub>)—The Simplest Unsaturated Geminal Diol—In Interstellar Analogue Ices. *J. Phys. Chem. Lett.* **2022**, *13*, 229–235.
- (27) Jones, B. M.; Kaiser, R. I. Application of Reflectron Time-of-Flight Mass Spectroscopy in the Analysis of Astrophysically Relevant Ices Exposed to Ionization Radiation: Methane (CH<sub>4</sub>) and D<sub>4</sub>-Methane (CD<sub>4</sub>) as a Case Study. *J. Phys. Chem. Lett.* **2013**, *4*, 1965–1971.
- (28) Turner, A. M.; Abplanalp, M. J.; Chen, S. Y.; Chen, Y. T.; Chang, A. H.; Kaiser, R. I. A Photoionization Mass Spectroscopic Study on the Formation of Phosphanes in Low Temperature Phosphine Ices. *Phys. Chem. Chem. Phys.* **2015**, *17*, 27281–27291.
- (29) Bouilloud, M.; Fray, N.; Bénilan, Y.; Cottin, H.; Gazeau, M. C.; Jolly, A. Bibliographic Review and New Measurements of the Infrared Band Strengths of Pure Molecules at 25 K: H<sub>2</sub>O, CO<sub>2</sub>, CO, CH<sub>4</sub>, NH<sub>3</sub>, CH<sub>3</sub>OH, HCOOH and H<sub>2</sub>CO. *Mon. Not. R. Astron. Soc.* **2015**, *451*, 2145–2160.
- (30) Pipes, J. G.; Roux, J. A.; Smith, A. M.; Scott, H. E. Infrared Transmission of Contaminated Cryocooled Optical Windows. *AIAA J.* **1978**, *16*, 984–990.
- (31) Roux, J.; Wood, B.; Smith, A.; Plyler, R. *Infrared Optical Properties of Thin CO, NO, CH<sub>4</sub>, HCl, N<sub>2</sub>O, O<sub>2</sub>, N<sub>2</sub>, Ar, and Air Cryofilms*; Technical Report, 1980.

- (32) Hudson, R. L.; Gerakines, P. A. Infrared Spectra and Interstellar Sulfur: New Laboratory Results for H<sub>2</sub>S and Four Malodorous Thiols. *Astrophys. J.* **2018**, *867*, 138.
- (33) Steele, B. D.; McIntosh, D.; Archibald, E. H.; Ramsay, W. IV. The Halogen Hydrides as Conducting Solvents. Part I.—The Vapour Pressures, Densities, Surface Energies and Viscosities of the Pure Solvents. Part II.—The Conductivity and Molecular Weights of Dissolved Substances. Part III.—The Transport Numbers of Certain Dissolved Substances. Part IV.—The Abnormal Variation of Molecular Conductivity, etc. *Philos. Trans. Royal Soc. A*. **1906**, *205*, 99–167.
- (34) Drouin, D.; Couture, A. R.; Joly, D.; Tastet, X.; Aimez, V.; Gauvin, R. CASINO V2.42 - A Fast and Easy-to-Use Modeling Tool for Scanning Electron Microscopy and Microanalysis Users. *Scanning* **2007**, *29*, 92–101.
- (35) Gerakines, P. A.; Schutte, W. A.; Greenberg, J. M.; van Dishoeck, E. F. The Infrared Band Strengths of H<sub>2</sub>O, CO and CO<sub>2</sub> in Laboratory Simulations of Astrophysical Ice Mixtures. *Astron. Astrophys.* **1995**, *296*, 810.
- (36) Chai, J.-D.; Head-Gordon, M. Long-range Corrected Hybrid Density Functionals with Damped Atom–Atom Dispersion Corrections. *Phys. Chem. Chem. Phys.* **2008**, *10*, 6615–6620.
- (37) Dunning, J.; Thom, H. Gaussian Basis Sets for Use in Correlated Molecular Calculations. I. The Atoms Boron Through Neon and Hydrogen. *J. Chem. Phys.* **1989**, *90*, 1007–1023.
- (38) Knizia, G.; Adler, T. B.; Werner, H.-J. Simplified CCSD(T)-F12 Methods: Theory and Benchmarks. *J. Chem. Phys.* **2009**, *130*, 054104.
- (39) Zhang, J.; Valeev, E. F. Prediction of Reaction Barriers and Thermochemical Properties with Explicitly Correlated Coupled-Cluster Methods: A Basis Set Assessment. *J. Chem. Theory Comput.* **2012**, *8*, 3175–3186.
- (40) Frisch, M.; Trucks, G.; Schlegel, H.; Scuseria, G.; Robb, M.; Cheeseman, J.; Scalmani, G.; Barone, V.; Mennucci, B.; Petersson, G.; et al. GAUSSIAN 16, Revision C.1; Gaussian Inc.: Wallingford, CT, 2019.
- (41) Werner, H.-J.; Knowles, P.; Lindh, R.; Manby, F. R.; Schütz, M.; Celani, P.; Korona, T.; Rauhut, G.; Amos, R.; Bernhardsson, A.; et al. MOLPRO, Version 2021.2, A package of ab initio programs; University of Cardiff: Cardiff, U.K., 2021. see: <http://www.molpro.net>.
- (42) Maity, S.; Kaiser, R. I.; Jones, B. M. Formation of Complex Organic Molecules in Methanol and Methanol–Carbon Monoxide Ices Exposed to Ionizing Radiation – a Combined FTIR and Reflectron Time-of-flight Mass Spectrometry Study. *Phys. Chem. Chem. Phys.* **2015**, *17*, 3081–3114.
- (43) Lignell, A.; Osadchuk, I.; Räsänen, M.; Lundell, J. Anharmonic Vibrational Spectrum and Experimental Matrix Isolation Study of Thioformic Acid Conformers—Potential Candidates for Molecular Cloud and Solar System Observations? *Astrophys. J.* **2021**, *917*, 68.
- (44) Wang, J.; Kleimeier, N. F.; Johnson, R. N.; Gozem, S.; Abplanalp, M. J.; Turner, A. M.; Marks, J. H.; Kaiser, R. I. Photochemically Triggered Chelotropic Formation of Cyclopropenone (c-C<sub>3</sub>H<sub>2</sub>O) from Carbon Monoxide and Electronically Excited Acetylene. *Phys. Chem. Chem. Phys.* **2022**, *24*, 17449–17461.
- (45) Milligan, D. E.; Jacox, M. E. Infrared Spectrum and Structure of Intermediates in the Reaction of OH with CO. *J. Chem. Phys.* **1971**, *54*, 927–942.
- (46) Hudson, R. L.; Moore, M. H. Laboratory Studies of the Formation of Methanol and Other Organic Molecules by Water + Carbon Monoxide Radiolysis: Relevance to Comets, Icy Satellites, and Interstellar Ices. *Icarus* **1999**, *140*, 451–461.
- (47) Bennett, C. J.; Hama, T.; Kim, Y. S.; Kawasaki, M.; Kaiser, R. I. Laboratory Studies on the Formation of Formic Acid (HCOOH) in Interstellar and Cometary Ices. *Astrophys. J.* **2011**, *727*, 27.
- (48) Turner, A. M.; Bergantini, A.; Koutsogiannis, A. S.; Kleimeier, N. F.; Singh, S. K.; Zhu, C.; Eckhardt, A. K.; Kaiser, R. I. A Photoionization Mass Spectrometry Investigation into Complex Organic Molecules Formed in Interstellar Analog Ices of Carbon Monoxide and Water Exposed to Ionizing Radiation. *Astrophys. J.* **2021**, *916*, 74.
- (49) Turner, A. M.; Koutsogiannis, A. S.; Kleimeier, N. F.; Bergantini, A.; Zhu, C.; Fortenberry, R. C.; Kaiser, R. I. An Experimental and Theoretical Investigation into the Formation of Ketene (H<sub>2</sub>CCO) and Ethynol (HCCOH) in Interstellar Analog Ices. *Astrophys. J.* **2020**, *896*, 88.
- (50) Jiménez-Escobar, A.; Chen, Y. J.; Ciaravella, A.; Huang, C. H.; Micela, G.; Cecchi-Pestellini, C. X-ray Irradiation of H<sub>2</sub>O + CO Ice Mixtures with Synchrotron Light. *Astrophys. J.* **2016**, *820*, 25.
- (51) de Barros, A. L. F.; Mejía, C.; Seperuelo Duarte, E.; Domaracka, A.; Boduch, P.; Rothard, H.; da Silveira, E. F. Chemical Reactions in H<sub>2</sub>O:CO Interstellar Ice Analogues Promoted by Energetic Heavy-ion Irradiation. *Mon. Not. R. Astron. Soc.* **2022**, *511*, 2491–2504.
- (52) Bennett, C. J.; Jamieson, C. S.; Osamura, Y.; Kaiser, R. I. A Combined Experimental and Computational Investigation on the Synthesis of [CH<sub>3</sub>CHO (X'A')] in Interstellar Ices. *Astrophys. J.* **2005**, *624*, 1097–1115.
- (53) Thi, W.-F.; van Dishoeck, E. F.; Dartois, E.; Pontoppidan, K. M.; Schutte, W. A.; Ehrenfreund, P.; d'Hendecourt, L.; Fraser, H. J. VLT-ISAAC 3–5 μm Spectroscopy of Embedded Young Low-mass Stars. *Astron. Astrophys.* **2006**, *449*, 251–265.
- (54) Charnley, S. B. Sulfuretted Molecules in Hot Cores. *Astrophys. J.* **1997**, *481*, 396–405.
- (55) van der Tak, F. F. S.; Boonman, A. M. S.; Braakman, R.; van Dishoeck, E. F. Sulphur Chemistry in the Envelopes of Massive Young Stars. *Astron. Astrophys.* **2003**, *412*, 133–145.
- (56) Cesaroni, R.; Beltrán, M. T.; Zhang, Q.; Beuther, H.; Fallscheer, C. Dissecting a Hot Molecular Core: the Case of G31.41+0.31. *Astron. Astrophys.* **2011**, *533*, A73.
- (57) Gibb, A. G.; Wyrowski, F.; Mundy, L. G. High-Velocity Gas Toward Hot Molecular Cores: Evidence for Collimated Outflows from Embedded Sources. *Astrophys. J.* **2004**, *616*, 301–318.
- (58) Martín, S.; Martín-Pintado, J.; Mauersberger, R.; Henkel, C.; García-Burillo, S. Sulfur Chemistry and Isotopic Ratios in the Starburst Galaxy NGC 253. *Astrophys. J.* **2005**, *620*, 210–216.
- (59) Martín, S.; Requena-Torres, M. A.; Martín-Pintado, J.; Mauersberger, R. Tracing Shocks and Photodissociation in the Galactic Center Region I. *Astrophys. J.* **2008**, *678*, 245–254.
- (60) Goto, M.; Geballe, T. R.; Indriolo, N.; Yusef-Zadeh, F.; Usuda, T.; Henning, T.; Oka, T. Infrared H<sub>3</sub><sup>+</sup> and CO Studies of the Galactic Core: GCIR 3 and GCIR 1W. *Astrophys. J.* **2014**, *786*, 96.